Accessing biochar's porosity using a new low field NMR approach and its impacts on the retention of highly mobile herbicides

Letícia de Pierri [a], Etelvino Henrique Novotny [b,1], Carlos Eduardo Pellegrino Cerri [a], Adijailton José de Souza [a], Bianca Braz Mattos [b], Valdemar Luiz Tornisielo [c], Jussara Borges Regitano [a,*]

[a] Luiz de Queiroz College of Agriculture (ESALQ), Dept. of Soil Science, University of São Paulo, Piracicaba, C.P. 09, 13418-260, SP, Brazil
[b] Brazilian Agricultural Research Corporation, Embrapa Soils, Rio de Janeiro, 22460-000, RJ, Brazil
[c] Center of Nuclear Energy in Agriculture (CENA), University of São Paulo, Piracicaba, 03178-200, SP, Brazil

HIGHLIGHTS

- A novel low field NMR-DDIF was successfully used to access biochar's porosity.
- Biochar's macropores and sorption enhanced with pyrolysis temperatures.
- SSA of pores with diameters >5.0 μm seemed to dictate biochar sorption.
- Herbicide aging enhanced sorption, but biochar granulometry did not.
- High biochar rate or proper incorporation is needed to retain mobile herbicides.

GRAPHICAL ABSTRACT
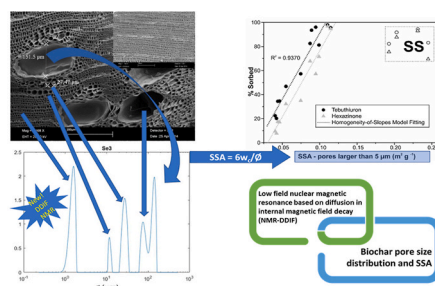
ARTICLE INFO

ABSTRACT

Agrowaste biochars [sugarcane straw (SS), rice husk (RH), poultry manure (PM), and sawdust (SW)] were synthesized at different pyrolysis temperatures (350, 450, 550, and 650 °C) to evaluate their potential to retain highly mobile herbicides, such as hexazinone and tebuthiuron that often contaminate water resources around sugarcane plantations. A new low field nuclear magnetic resonance approach based on decay due to diffusion in internal magnetic field (NMR-DDIF) was successfully used to determine biochar's porosity and specific surface area (SSA) to clear the findings of this work. SSA of pores with diameters >5.0 μm increased with pyrolysis temperatures and seemed to dictate biochar's retention, which was >70% of the applied amounts at 650 °C. These macropores appear to act as main arteries for herbicide intra-particle diffusion into smaller pores, thus enhancing herbicides retention. Biochar granulometry had little, but herbicide aging had a significant effect on sorption, mainly of tebuthiuron. However, soils amended with 10,000 kg ha^{-1} of the biochars showed low sorption potential. Therefore, higher than usual biochar rates or proper incorporation strategies, i.e., surface

incorporation, will be needed to remediate areas contaminated with these highly mobile herbicides, thus precluding their leaching to groundwaters.

1. Introduction

Amending soils with biochar has several agricultural and environmental potential advantages, such as enhancement of soil cation exchange capacity (CEC); pH; organic carbon (OC) content; microbial activity; and water holding capacity, besides promoting remediation of contaminated soils (Wang et al., 2021). Biochar is a promising sorbent for pesticides as well as other organic pollutants (Egbosiuba et al., 2020; Hassan et al., 2020; Liu et al., 2018; Siedt et al., 2021), thus decreasing their availability and subsequent leaching to groundwaters (Khorram et al., 2017; Mandal et al., 2017a). Conversely, higher retention implies in higher pesticide application rates to guarantee pest control (Novotny et al., 2015), mainly for pre-emergent molecules, which may offset biochar advantages.

Most reports on sorption of pesticides to soils amended with biochar regarded only molecules having low to moderate mobility (Delwiche et al., 2014; Deng et al., 2017; Mandal et al., 2017b; Wang et al., 2016), posing little risks of leaching to groundwaters (Cabrera et al., 2014). The rare reports with highly mobile molecules suggest that biochar is not efficient in their retention (Cabrera et al., 2014; Dechene et al., 2014; Rittenhouse et al., 2014; Yavari et al., 2016). Tebuthiuron and hexazinone are good examples of highly mobile herbicides that have high persistence in soils (12–15 and 9 months, respectively) and may reach water resources (Mendes et al., 2021). They are widely used in the world, especially in Brazil, to control weeds associated with sugarcane plantations and are often detected in groundwaters (Albuquerque et al., 2016; Cerdeira et al., 2005). This is an important issue since Brazil yielded 616 million tons of sugarcane in an area of 8.4 million of ha in 2019/2020, including the recharging areas of Guarany Aquifer.

Hydrophobic partitioning is one of the main mechanisms involved in pesticide sorption to biochars (Inyang and Dickenson, 2015; Liu et al., 2018; Wang et al., 2016). However, pesticide interactions with the biochar matrix are quite complex, depending on their both physical-chemical attributes (Siedt et al., 2021), such as solubility and ionization constant of the pesticide, hydrophobic/hydrophilic moieties of both pesticide and biochar, as well as other biochar's attributes, such as specific surface area (SSA), oxidation degree, aromaticity, porosity (size and amount), carbon content, and pH (Conz et al., 2017; Egbosiuba et al., 2020; Liu et al., 2018; Mandal et al., 2017a; Sun et al., 2012), which are directly affected by feedstock origin and pyrolysis conditions (Hassan et al., 2020; Novotny et al., 2015). SSA is claimed to be a key biochar factor dictating pesticide retention (Li et al., 2017; Mandal et al., 2017a), but pore volume and its geometry also seem to play an essential role (Mandal et al., 2017a; Xiao and Pignatello, 2015). However, other mechanisms, such as co-precipitation, specific surface adsorption, and physisorption (sequestration or pore filling) can also take place (Hassan et al., 2020; Jin et al., 2016).

In such complex systems, sorption should not reach equilibrium at short periods. The literature neglects the effects of pesticide residence time (hereafter mentioned as "pesticide aging") on its sorption to biochars, focusing mainly on biochar's aging effects (Liu et al., 2018). However, pesticide's aging dictates its environmental fate and the risks associated with its use (Boesten, 2017). Biochar granulometry should also affect pesticide sorption since grinding enhances contact surface area (Kang et al., 2018). However, field application of pulverized biochar is troubled by wind spreading (Gao and Wu, 2013; Gelardi et al., 2019).

Quantifying biochar's porosity and SSA is a challenge due to its wide pore size range and methodological issues, such as sample changes during degasification (BET) or sample crushing (mercury porosimetry) (Brewer et al., 2014). The use of NMR relaxometry, probing relaxivity dependent modes (T_1 and/or T_2 ground modes) to estimate the porosity (Conte et al., 2014; De Pasquale et al., 2012; Wong et al., 2019), also fails since decay signals are function of two incognitos, pore size and surface relaxivity. Besides, surface relaxivity is regarded as uniform and homogeneous across all different pore size classes (Benavides et al., 2020), an unlike premise for natural porous materials (Liu et al., 2014; Benavides et al., 2017, 2020, 2020).

A method based on diffusion modes instead of relaxivity modes, using field inhomogeneity (internal magnetic field gradient) due to natural susceptibility contrast in the sample, was previously proposed by Song and collaborators (Song et al., 2000; Song, 2003). The key point to this methodology is that diffusion decay signals are governed only by pore size. The authors provided an elegant, clear, and detailed explanation of this phenomenon and its application to access pore sizes of glass beds and natural rocks, which is beyond our scope. However, our work was the first in the literature to use this methodology to determine biochar pore size distribution.

The main goal of this research was to evaluate the effects of agrowaste biochar sources and pyrolysis temperatures, as well as herbicide aging and biochar granulometry, on the sorption of hexazinone and tebuthiuron, both considered highly mobile herbicides ($K_d > 5\,L\,kg^{-1}$). Due to our difficulties with traditional methods, a new low field nuclear magnetic resonance method was developed to determine biochar pore sizes, using, for the first time, decay due to diffusion in internal magnetic field method (NMR-DDIF). It was hypothesized that: *ii)* feedstock and pyrolysis temperature affect biochar physical-chemical attributes, mainly its porosity and SSA, and dictate its sorption potential; *ii)* amending soils with agrowaste biochars having high sorption potential should be an efficient strategy to remediate leaching of highly mobile herbicides; *iii)* herbicide aging and finer biochar granulometry will further enhance these herbicides sorption in biochar amended soils; and *iv)* NMR-DDIF is able to determine biochar's pore size distributions.

2. Materials and methods

2.1. Soil attributes

Soil samples were collected at 0–10 cm layer from two conventional sugarcane plantations, in a sandy loam Arenic Hapludult located at 22°42′59″S 47°48′05″W and in a clay Rhodic Hapludox located at 22°44′00″S 47°33′12″W, as well as from an organic sugarcane plantation in a sandy clay Rhodic Hapludox located at 21°11′27″S 48°07′46″W. The samples were air-dried, 2-mm sieved and stored at 4 °C. Granulometry was measured by the densimeter method (Teixeira et al., 2017); chemical attributes (pH, $H^+ + Al^{3+}$, and K^+, Ca^{2+}, and Mg^{2+}) were evaluated as in Raij et al. (2001); and total C by wet oxidation (Teixeira et al., 2017), which are summarized in Table 1. Dissolved organic carbon (DOC) was extracted in the biochar amended soils with ultrapure water (0.055 μS

Table 1
Soil physical-chemical attributes.

Attributes [a]	Soils		
	Sandy loam	Sandy clay	Clay
Sand (g kg⁻¹)	888	476	84
Silt (g kg⁻¹)	10	68	360
Clay (g kg⁻¹)	101	456	556
pH	6.0	6.3	5.9
CEC (mmol_c dm⁻³)	56	79	76
V (%)	76	74	64
Total C (g kg⁻¹)	5.0	16.3	15.3

[a] CEC = cation exchange capacity; V = base saturation.

cm^{-1}), and DOC contents were measured by dry combustion (Shimadzu-5000 A, non-dispersive infrared) after filtering the supernatants in calcined fiberglass (<0.7 μm) (Table S1).

2.2. Biochars' manufacture and attributes

Biochars were produced by slow pyrolysis in a hermetically sealed reactor. Briefly, feedstocks [sugarcane straw (SS); rice husk (RH); poultry manure (PM); and sawdust (SW)] were dried at 105 °C and placed in the reactor saturated with N$_2$, in which temperature was raised at 10 °C min^{-1}, during 30 min, and then 20 °C min^{-1} for 15 min up to final temperatures (350, 450, 550, and 650 °C), which were chosen to contemplate all steps of cellulose, hemicellulose, and lignin thermal decomposition, besides being compatible with values from the literature. Then, the biochars were removed 12 h after the reaction's completion (after stopping gas release from the reactor and cooling sample holder), ground and sieved at 0.15 mm and 2 mm meshes or kept at original sizes (>2 mm). Scanning electron microscopy (SEM) images (LEO 435VP) were collected by taking transversal sections after gold covering the samples (Sputter SCD 050 Baltec), which were preserved in liquid-N$_2$. Further information on biochar manufacturing and attributes is fully detailed in Conz et al. (2017) and summarized in Table S2.

At first, measurements of biochar's pore volume (porosity) and SSA were tried using N$_2$-adsorption/desorption isotherms (BET and BJH methods), as recommended by the biochar characterization guideline (IBI, 2015), but it did not provide reliable results since mean standard deviations were too high (Table S3) (Sun et al., 2012). Application of BET theory to microporous materials is questionable since it is based on gas adsorption-desorption on flat surfaces (Mukhtar et al., 2020). It also entails degasification, which often requires sample heating that leads to release of condensable volatiles, thus altering porosity (Brewer et al.,

2014). Therefore, biochar's pore size distribution and SSA were estimated for the first time by NMR-DDIF methodology (Liu et al., 2014; Song, 2003; Song et al., 2000).

To validate this methodology, a set of random loose packings of monosized beads (glass microspheres), having different radii (R_{bead}: 10, 25, and 60 μm) were employed. In this case, pore size can be estimated assuming that the pore radius (R_{pore}) ≈ 0.45 R_{bead} (Rémond et al., 2008), which corresponded to 4.5, 11.3, and 27.0 μm, respectively. In addition, four artificial sintered sand-glass samples having different pore sizes (30; 39; 80 and 100 μm, determined by microtomography) were kindly provide by Chencarek (Chencarek et al., 2019; Chencarek, 2021). In brief, the samples were water saturated at 33 °C (the magnet operational temperature), placed in a sealed polyethylene bag (ordinary plastic bag) to avoid water evaporation and analyzed at low field NMR spectrometer (Specfit H50 benchtop NMR spectrometer, Fine Instruments Technology), with a permanent magnet of 0.35 T (^{1}H Larmor frequency of 15 MHz). The two pulse sequences, that measure pore size distribution from DDIF, used adjusted encoding time (t_e), according to Lisitza and Song (2001), and 50 delays in relation to the observation time for molecular diffusion (t_{diff}) logarithmically spaced from 1 μs to 3 s (Song, 2003). For each t_{diff} step, 8 scans were performed. All the NMR experiments were performed using a recycle delays at least five times longer than the ^{1}H spin-lattice relaxation time (T_1), as determined by previous inversion-recovery experiments.

After method validation (Figs. 1 and 2), biochar pore size distribution was measured by taken ~5 g samples and saturating them with distilled water in spin-filters (maxi-spin filter tubes, 25 mL). Then, they were thermalized at 33 °C and analyzed at low field NMR spectrometer as described above. The encoding time (t_e = 1.5 ms) was determined according to Lisitza and Song (2001). To quantify the water content inside the porous, the Carr-Purcell-Meiboom-Gill train pulse (CPMG) was employed. The pore size distribution (from DDIF experiments), as
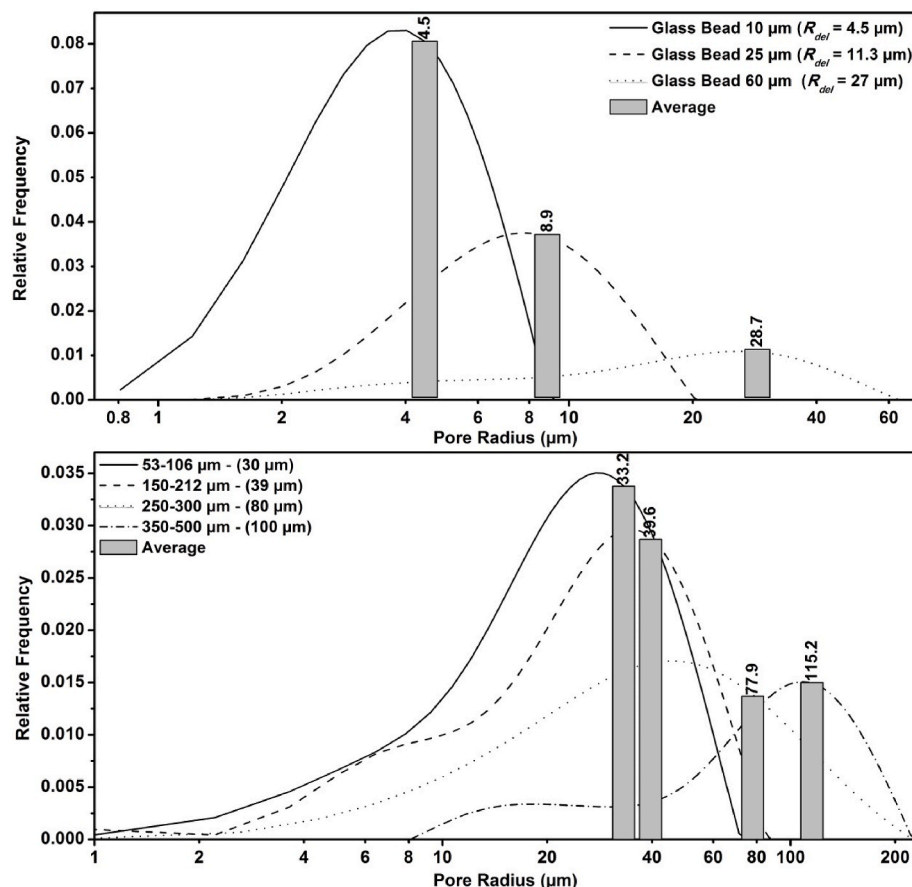

Fig. 1. Pore size distribution obtained from NMR-DDIF. Upper panel: glass beads with different radii (10; 25 and 60 μm), having R_{del} (Delaunay empty spheres radius) = R_{pore} (pore radius) ≈ 0.45 R_{bead} (bead radius) (Rémond et al., 2008). Lower panel: synthetic porous samples obtained by sintering solid glass microspheres of four different grain size ranges (53–106 μm; 150–212 μm; 250–300 μm; and 350–500 μm) (Chencarek et al., 2019). The values between parentheses refer to average pore size radius estimated from 2D Micro-Tomography Images (Chencarek, 2021). For both panels, the gray columns and their labels represent the average pore size of the obtained distribution by NMR-DDIF.
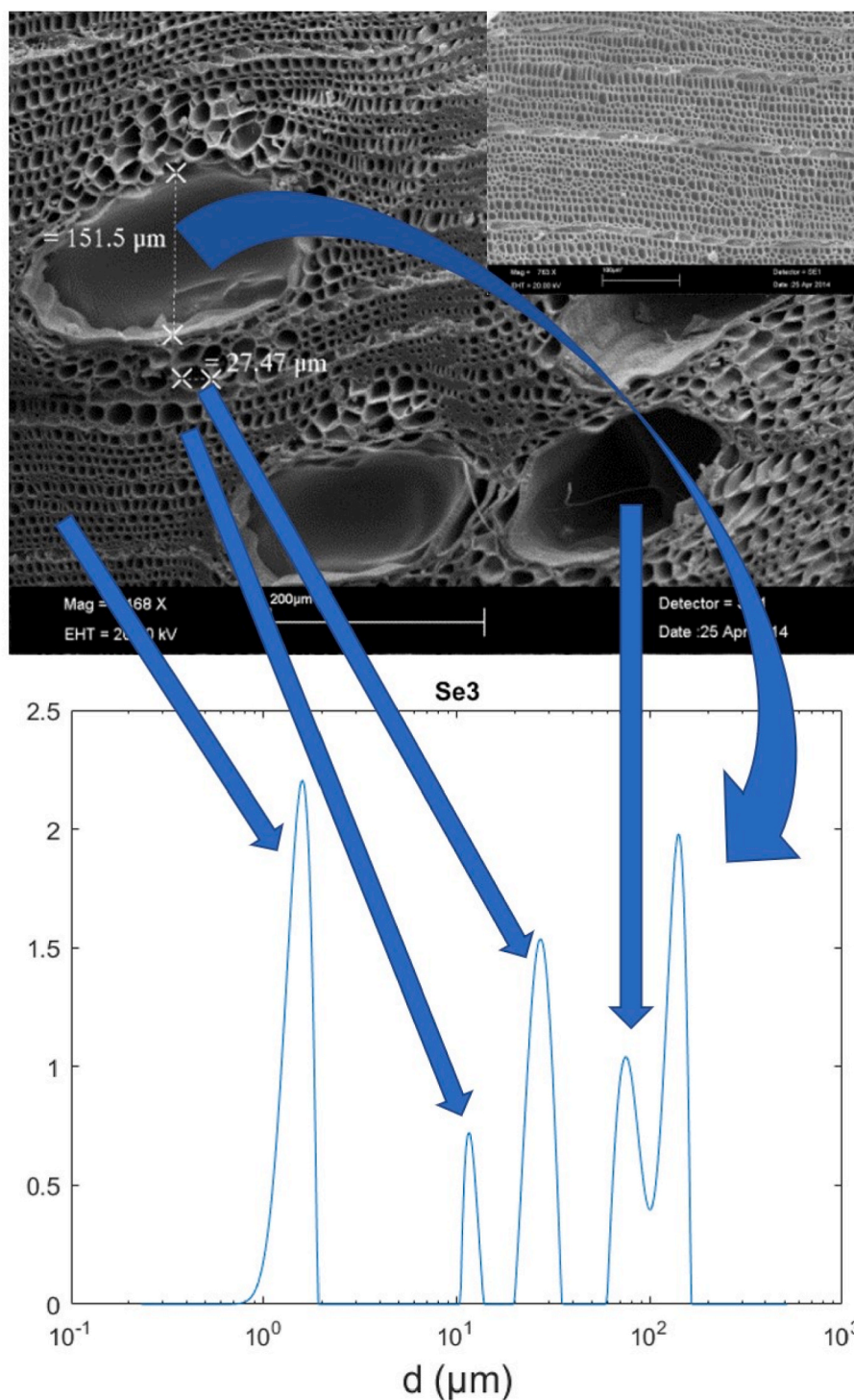
Fig. 2. Example of qualitative comparison between Scanning Electron Microscopy (SEM) and Low-Field Nuclear Magnetic Resonance Spectroscopy (NMR) using the Decay due to Diffusion in Internal magnetic Field (DDIF) methodology. Sample: SW550. d is the pore diameter.

well as the transverse relaxation time (T_2) distribution, were obtained after the Inverse of Laplace Transform (ILT) of the obtained decays. The total ILT area of CPMG experiment was linearly proportional to the water content in the samples ($R^2 = 0.9999$, n = 25). For the estimation of the water into the porous system only (*i.e.*, total water accessible pore volume), the free water signal (longest T_2) was excluded from the ILT-area calculation. Knowing the water content within the pores (CPMG) and their diameters (DDIF), the specific surface area determined by NMR (NMR-SSA) is easily obtained considering spherical pores, which is a realistic premise based on SEM images (Fig. 3).

2.3. Sorption to biochars

Sorption coefficients were called apparent ($K_{d,app}$) since they were evaluated at just one concentration based on our previous works showing that tebuthiuron (*N*-[5-(1,1-dimethylethyl)-1,3,4-thiadiazol-2-yl]-*N*,*N'*-dimethylurea) [water solubility (S_w) = 2.5 g L^{-1} and soil distribution coefficient (K_d) = 0.002–3.6 L kg^{-1}] and hexazinone (3-cyclohexyl-6-dimethylamino)-1-methyl-1,3,5-triazine-2-4(1H, 3H)-dione) (S_w = 33 g L^{-1} and K_d = 0.07–1.65 L kg^{-1}) isotherms were close to linearity (Toniêto et al., 2016). Their equilibrium was reached in 24 h and they did not
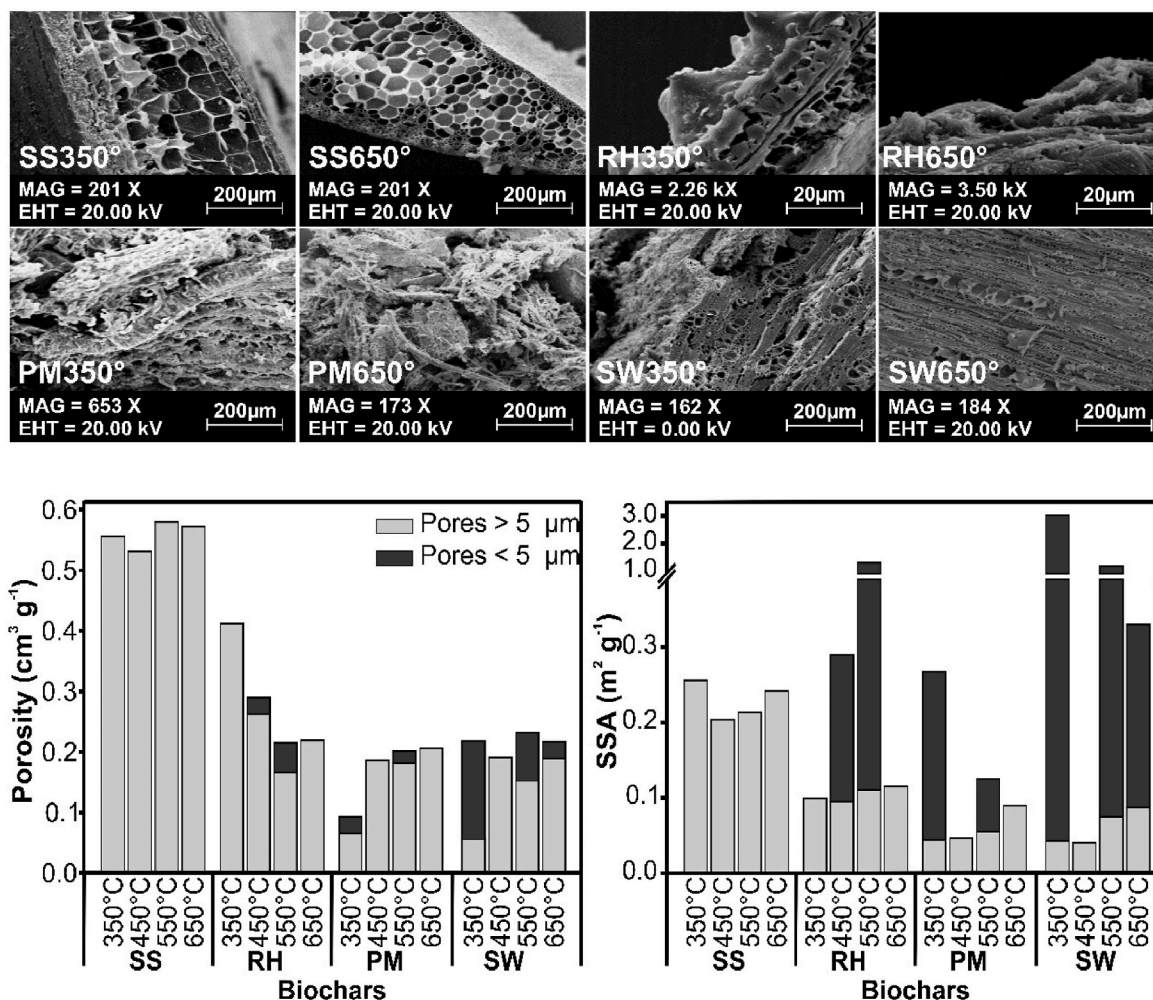
4

Fig. 3. Scanning electron microscopy (SEM) images of sugarcane (SS), rice husk (RH), poultry manure (PM) and sawdust (SW) biochars as affected by pyrolysis temperatures (350 and 650 °C). Lower panels: biochar's porosity (cm³ g⁻¹) and specific surface area (m² g⁻¹) measured by low field NMR-DDIF.

degrade during experiment duration (24 h) (Pereira-Junior et al., 2015; Toniêto et al., 2016).

So, aliquots of 500 mg of biochar and 25 mL of herbicide solutions were added to centrifuge tubes (Teflon, 50 mL). These solutions had final concentrations equal to 0.04 and 0.08 µg mL⁻¹ (corresponding to 1.9 and 3.8 µg g⁻¹ of biochar) for hexazinone and tebuthiuron, respectively, and were prepared in aqueous CaCl₂ 0.005 mol L⁻¹ to simulate soil solution ionic strength. They both were spiked with ¹⁴C-labelled molecules (¹⁴C-URL-molecules, purities >98%, and specific activities equal to 3.14 and 3.01 MBq mg⁻¹ for hexazinone and tebuthiuron, respectively), thus reaching final radioactive concentrations equal to 0.12 kBq mL⁻¹. Then, the tubes were horizontally shaken at 200 rpm for 24 h, and centrifuged at 4,711*g* for 10 min at 4 °C (OECD, 2000). After, 1 mL aliquots of the supernatants were taken and quantified by liquid scintillation spectroscopy (LSS) (Packard Tri-Carb 2200 LSA, PerkinElmer) to determine equilibrium solution concentration (C$_e$). The sorption study was performed in duplicates, in a completely randomized design. Sorbed amounts (S) were calculated by the difference between initial concentration (C$_i$) and C$_e$, considering the biochar (mass): solution (volume) ratio. Then, apparent sorption coefficients were calculated as K$_{d,app}$ = S/C$_e$.

2.4. Sorption to biochar amended soils

Aliquots of 5 g of soil, 38.4 mg of biochars (calculated assuming an application rate of 10,000 kg ha⁻¹, soil density of 1.3 g cm⁻³, and soil depth of 10 cm), and 10 mL of 0.2 and 0.4 µg mL⁻¹ (corresponding to 0.4 and 0.8 µg g⁻¹ of soil) of hexazinone and tebuthiuron solutions, respectively, dissolved in aqueous CaCl₂ 0.005 mol L⁻¹, were added to centrifuge tubes (Teflon, 50 mL). These solutions were also spiked with ¹⁴C-labelled molecules and reached final radioactive concentrations equals to 0.12 and 0.18 kBq mL⁻¹, respectively. Then, the tubes were shaken, centrifuged, and analyzed by LSS and K$_{d,app}$ was calculated as mentioned in section 2.3.

2.5. Sorption as affected by herbicide aging and biochar granulometry

The PM350 and SS550 as well as the sandy loam and clay soils were selected due to their contrasting sorption behaviors.

At first, 5 g of the above biochar (at sizes <0.15, <2, and >2 mm) amended soils were weighed, placed in Teflon tubes (50 mL), and moistened to 70% of field capacity. Then, aliquots of 100 µL ¹⁴C-herbicide solutions were added at the same application rates as mentioned in section 2.4. Then, aliquots of 10 mL CaCl₂ 0.005 mol L⁻¹ were added to the tubes either immediately (T₀) or 15 d after the herbicide application (T₁₅), which was arbitrarily chosen to simulate aging; the aged tubes (T₁₅) were incubated in a semi-dark room at 25 ± 2 °C. Soil and biochar masses, shaking period, and centrifuging conditions were performed as described in section 2.3. However, the sorbed amount (S) was evaluated by combustion (OECD, 2000 modified). For this, soil slurries were dried at 40 °C, macerated in a porcelain mortar, and triplicates of 0.2 g were taken for combustion at 900 °C for 3 min, using a biological

oxidizer (Biological Oxidizer OX-500, R.J. Harvey Instrument Corporation). Then, the $^{14}C–CO_2$ evolved from herbicide combustion was trapped in monoethanolamide solution and quantified by LSS. Recoveries ranged from 86 to 105% of the respectively applied radioactivities (AR) and $K_{d,app}$ was calculated as in section 2.3.

2.6. Analyses of the results

Residue's normality (Shapiro-Wilk test) and homoscedasticity (Bartlett test) were tested and graphically evaluated after analysis of variance ($p < 0.05$) for each herbicide. When necessary, the dataset was log-transformed according to the Box-Cox technique. Interactions among factors (soil, biochar, aging, and granulometry) were evaluated using R® statistical software and the confidence intervals (CI, α = 95%) were calculated for each herbicide model by linear regression to differentiate treatments. CI was chosen to provide visual and conservative pairwise comparison. Also, the main factors were evaluated by marginal distribution graphs.

3. Results

3.1. NMR-DDIF method validation

Average pore radius values (grey columns) obtained by NMR-DDIF were in very good agreement with the expected values (values between parentheses) for all samples (Fig. 1). These results corroborate with those obtained for glass beads and rock cores by Song et al. (2000); Lisitza and Song (2001); and Song (2003). Furthermore, the qualitative comparisons between pore sizes from scanning electron microscopy (SEM) and those obtained by NMR-DDIF were also very consistent (Fig. 2). Therefore, the use of this methodology is valid to analyze pore size distribution of biochars in a relevant scale for the studied samples (from few to hundreds μm).

3.2. Summary of biochar attributes

All biochars presented high pH values (7.5–9.9) (Table S2). The wood-based biochar (SW) showed the lowest electrical conductivities (EC) and ash contents, but the highest total-C and fixed-C contents. An opposite trend was observed for the manure-based biochar (PM). Total-C was also high for the straw-based biochar (SS), which seemed to have similar features to SW. Except for having lower CEC, the husk-based biochar (RH) resembled PM. Overall, CEC tended to decrease, whereas total-C tended to increase with pyrolysis temperature.

Biochars differed on morphological structures depending on their feedstock and pyrolysis temperature (SEM images, Fig. 3). In addition, pore size distribution and SSA were successfully determined by low field NMR-DDIF method, unprecedented for biochar characterization (Figs. 1–3). According to it, SS showed higher porosity and SSA of porous >5 μm. RH presented intermediate pore volume and pore size; most porosity is placed mainly in the epicarp tissue that seems to collapse at the highest pyrolysis temperature. PM did not show a visible pore network by SEM, but they were at some extent quantified by NMR-DDIF that showed a quite disform pore distribution, likely due to the greater representativeness of the sample by NMR-DDIF than by SEM. SW showed the same pore volume as PM, but their pore sizes were smaller and relatively uniformly distributed. Plant cells' regular size and arrangement in most woody biomasses result in biochars having discrete groups of pores, with similar sizes and rather regular spatial arrangement (Sun et al., 2012). Poultry manure and SW exhibited the lowest pore volume and SSA of porous >5 μm (Fig. 3).

3.3. Sorption to biochars

Regardless of the biochar pyrolysis temperatures, both herbicides were highly sorbed to SS and RH (S ≥ 72 and 81% of the applied

radioactivity (AR) and $K_{d,app}$ ≥ 126 and 216 L kg^{-1} for hexazinone and tebuthiuron, respectively) (Fig. 4 and Fig. S1). They were less sorbed to PM and SW, mainly at lower pyrolysis temperatures (≤550 °C) (S ≤ 35 and 57% of AR and $K_{d,app}$ ≤ 30 and 68 L kg^{-1}, respectively) (Fig. 4 and Fig. S1). Sorption of these highly mobile herbicides enhanced with pyrolysis temperatures, especially for PM and SW.

3.4. Sorption to biochar amended soils

Biochar amendments increased hexazinone and tebuthiuron sorption, except for PM350 and all SW (Fig. 5, Table S4). Sorption enhancement was most conspicuous for the soil with lowest clay and organic matter contents (sandy loam), thus having the lowest buffer capacity (Fig. 5, Table 1 and Table S4). However, sorption coefficients of both herbicides were still low even after biochar amendments: $K_{d,app}$ ≤ 1.10 L kg^{-1} (≤32% of AR) for hexazinone and $K_{d,app}$ ≤ 3.76 L kg^{-1} (≤63% of AR) for tebuthiuron (Fig. 5 and Fig. S2).

Biochar pyrolysis temperatures did not affect hexazinone and tebuthiuron sorption to soils amended with SS and SW, but it enhanced their sorption to soils amended with RH and especially with PM (Fig. 5). For RH, sorption enhancement was observed only up to 550 °C.

3.5. Sorption as affected by herbicide aging and biochar granulometry

Sorption to biochar amended soils increased when herbicides were aged for 15 d, especially for tebuthiuron and SS (Fig. 6). Aged $K_{d,app}$ values were consistently low for hexazinone (≤3.31 L kg^{-1}), but reached moderate values for tebuthiuron (5.00–8.03 L kg^{-1}).
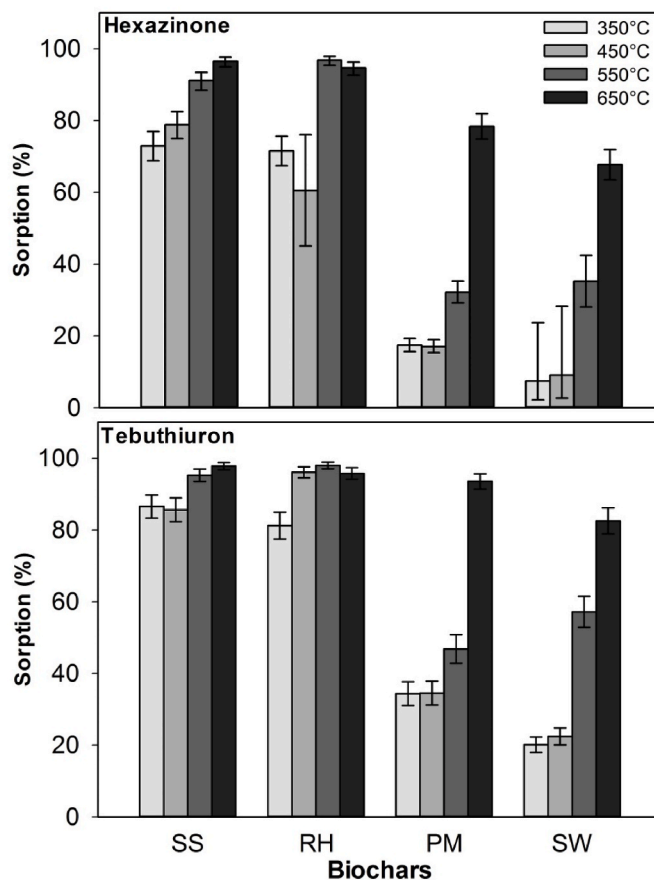

Fig. 4. Effects of biochar sources [sugarcane straw (SS); rice husk (RH); poultry manure (PM); and sawdust (SW)] and pyrolysis temperatures (350, 450, 550, and 650 °C) on the sorption of hexazinone and tebuthiuron. Error bars indicate modeled confidence interval (α = 95%).
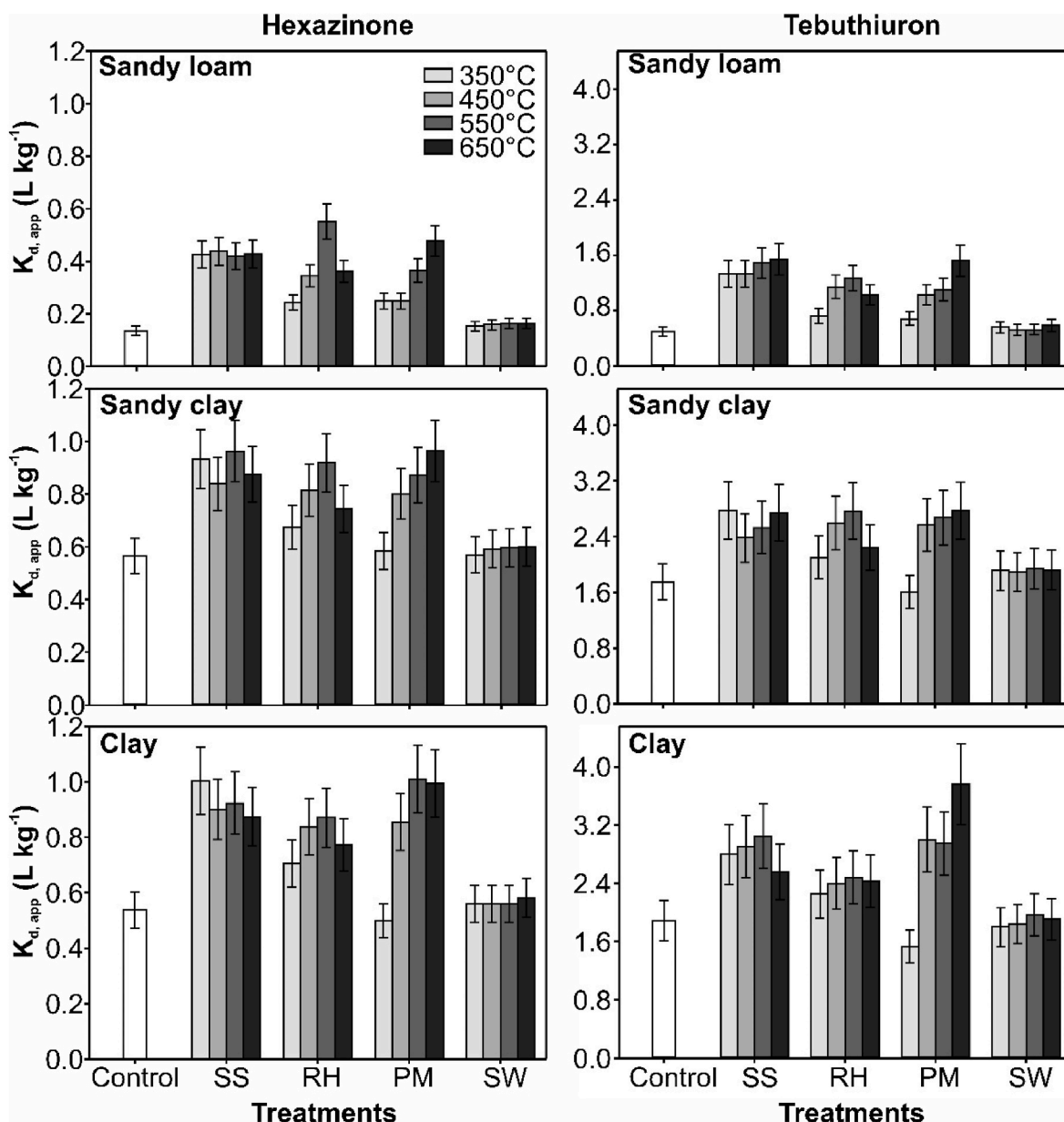
Fig. 5. Apparent sorption coefficients ($K_{d,app}$) for hexazinone and tebuthiuron as affected by biochar sources, pyrolysis temperatures, and soil types. Error bars indicate modeled confidence interval ($R^2 = 0.98$ for both molecules; $\alpha = 95\%$).

The effects of herbicide's aging on sorption were more pronounced than their granulometry, but sorption was generally higher for finer aged biochars (<0.15 mm at T_{15}) (Fig. 6). Sorption quantification for coarser biochars (>2 mm) was less precise, showing higher standard deviations than for the finer ones.

4. Discussion

4.1. Sorption to biochars

Sorption trends for hexazinone and tebuthiuron showed the same patterns, they were only different in magnitudes. Therefore, they will be primarily discussed together.

Pesticide retention to biochars is quite complex. Hydrophobic partition is often mentioned as the major mechanism involved, in analogy to pesticide sorption to soils (Hassan et al., 2020; Inyang and Dickenson, 2015; Liu et al., 2018; Wang et al., 2016). It means that pesticide should partition into hydrophobic fractions of the biochar, such as polyaromatic

backbone and hydrophobic condensed hydrocarbons. Here, SW showed the highest C content but the lowest sorption potential, suggesting that other mechanisms related to biochar's structure or composition nature should be involved.

For biochars, pore filling and intra-particle diffusion are highly regarded since sorption is always related to pore structures, either amounts, sizes, or SSAs (Tan et al., 2015; Xiao and Pignatello, 2015). In the literature, micro (<2 nm) and meso (2–50 nm) pores are claimed to control almost entirely the interactions between fluid molecules and pore walls (Lowell et al., 2004), but macropores, not accessible by BET (Brewer et al., 2014; Wong et al., 2019), may act as main arteries for intra-particle diffusion to meso and micropores. Gray et al. (2014) have already pointed that IUPAC's pore size classification system did not adequately describe larger biochar pore sizes that may dominate water retention. It seems that "larger pores" play a crucial role in modulating herbicide interactions between aqueous phase and biochar surfaces that drive important biochar hydraulic properties related to herbicide retention and its subsequent environmental fate (Sun et al., 2012). It
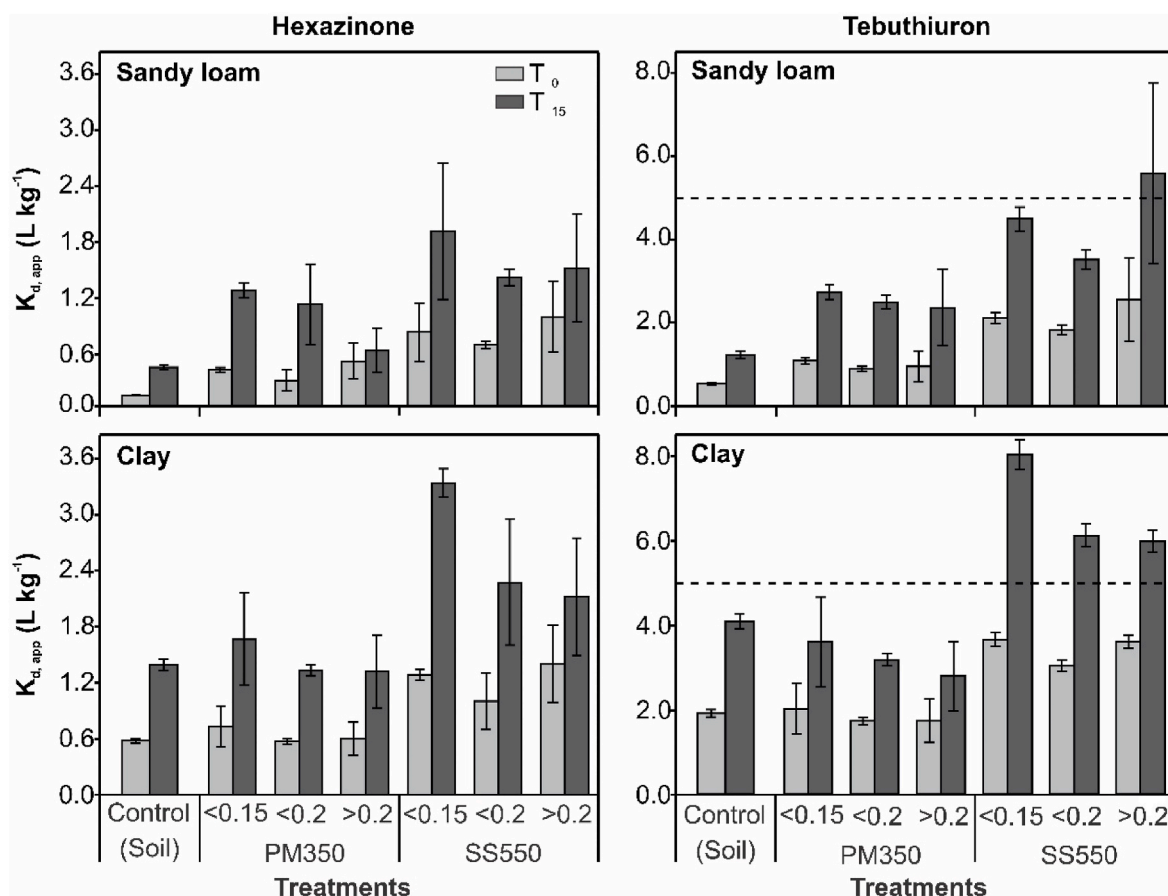
Fig. 6. Apparent sorption coefficients ($K_{d,app}$) for hexazinone and tebuthiuron as affected by herbicides aging ($T_0 = 0$ and $T_{15} = 15$ d after herbicides application) and biochars granulometry (<0.15 mm, < 2 mm, and > 2 mm) in a sandy loam and a clay soil. The horizontal dotted line is referred to the leaching class ($K_{d,app} > 5$ L kg^{-1}: non-leachable; $K_{d,app} < 5$ L kg^{-1}: leachable). Error bars indicate modeled confidence interval ($\alpha = 95\%$).
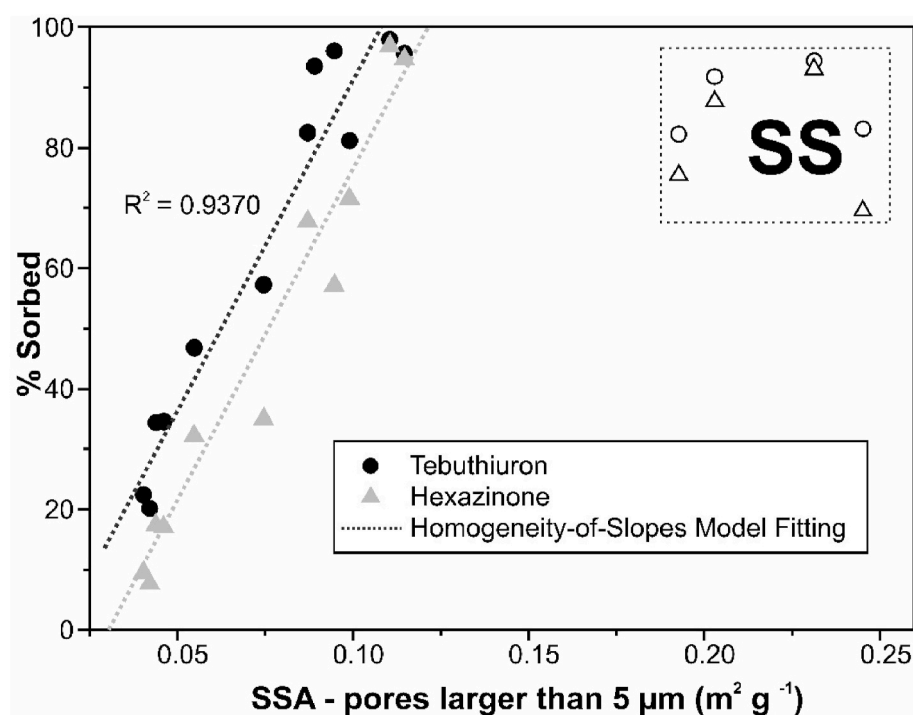

Fig. 7. General linear regressions between NMR-SSA for pores larger than 5 μm and percentages of hexazinone and tebuthiuron sorbed to agrowaste biochars [sugarcane straw (SS); rice husk (RH); poultry manure (PM); and sawdust (SW) pyrolyzed at 350, 450, 550, and 650 °C].

should play even major role for hydrophilic molecules, such as hexazinone and tebuthiuron.

The above assumption is ratified by the fact that both herbicide retentions to biochars were highly correlated with SSA of pores having diameter >5.0 μm ($R^2 = 0.94$ and $p < 0.001$) when determined by low field NMR-DDIF, except for SS (Fig. 7). However, a poor fitting was observed when the SSAs of smaller pores (diameter <5.0 μm) were included ($R^2 = 0.10$ and 0.12 for hexazinone and tebuthiuron, respectively, and $p > 0.25$). It was likely due to either steric hindrance accessing tiny pores as pointed for other triazine herbicides (Xiao and Pignatello, 2015), or to a strong leverage of SW since it presents the largest amount of tiny pores (<5.0 μm, Fig. 3) but unexpected low sorption (Fig. 4). The model fit improved considerably after excluding pores <5.0 μm since contribution of SW to sorption was minimized. Besides, the sensibility of DDIF method is poor for these tiny pores, since the lowest pore size limit, using water as a probe, is given by d $> \sqrt{2.6519\,t_e} \sim 2$ μm (Song, 2003). These hypotheses will be evaluated in upcoming studies.

The SSs presented markedly higher SSA for pores >5 μm (Fig. 3), suggesting that they should be capable of retaining more herbicides than their applied amounts (regarded equal to 100%) (Fig. 4), thus configuring as an outlier to the general model (Fig. 7). It means that either SS extra retention was squandered since almost all the applied herbicide was already sorbed, or part of the SS porous system was unavailable to herbicides sorption. Further studies including higher herbicide rates as well as different sorbent/sorbate ratios and probes are needed to clarify this.

4.2. Sorption to biochar amended soils

Soils with higher clay and OC contents (sandy clay and clay) presented higher herbicide sorption. In addition, biochar amendments enhanced herbicide sorption to soils, except for PM350 and SW. The SSs, RH550, and PM650 were the most whereas SWs were the least efficient promoting sorption. The formers had higher SSA >5 μm capable of retaining highly mobile herbicides or to favor their diffusion to deeper and smaller pores with subsequent sequestration (Sun et al., 2012; Xiao and Pignatello, 2015). The SWs presented higher total and fixed-C contents as well as higher aromaticity, but their amendments to soils did not enhance sorption, ruling out hydrophobic partition as a major sorption mechanism (Ahmad et al., 2014; Inyang and Dickenson, 2015; Oliveira et al., 2017; Wang et al., 2016). Hardwood biochars may sterically hinder diffusion of herbicides, such as triazines (Xiao and Pignatello, 2015).

RH and PM amendments to soils generally enhanced sorption, especially at higher pyrolysis temperatures (Fig. 5). In spite their different composition, since RHs are composed mostly of lignin ($>85\%$) whereas PMs are composed mostly of hemicellulose (37–50%) and lignin (40–52%) (Conz, 2015), their SSAs of pores >5 μm increased with pyrolysis temperatures and favored sorption. Atypically, amending PM350 to soils leveled or decreased sorption but doubled dissolved organic carbon (DOC) contents in the soil solution. DOC may act as a co-solvent for organic molecules, such as pesticides (Haberhauer et al., 2002), inhibiting their sorption. This effect should have been obfuscated at higher pyrolysis temperatures by the enhancements in their SSA of pores >5 μm. Amending RH650 slightly decreased sorption in relation to RH550 likely due to the collapse of at least part of larger epicarp pores when manufactured at 650 °C (Ahmad et al., 2014; Kookana, 2010).

Sorption enhancements resulted from biochar amendments were not enough to turn hexazinone and tebuthiuron non-leachable in the soils ($K_{d,app} < 5.0$ L kg^{-1}). Similar results were observed for other highly mobile pesticides, such as aminocyclopyrachlor and imazapic and imazapyr as well as chloridazon and metazachlor metabolites (Dechene et al., 2014; Rittenhouse et al., 2014; Yavari et al., 2016). Nevertheless, biochar enhanced sorption of moderately soluble molecules, such as atrazine, imidacloprid, isoproturon, and fomesafen (Delwiche et al., 2014; Deng

et al., 2017; Jin et al., 2016; Khorram et al., 2017), but not of those having low mobility, such as glyphosate and paraquat (Cabrera et al., 2014; Herath et al., 2016; Tsai and Chen, 2013). Here, the biochars were applied at 10,000 kg ha^{-1} rate (c.a. 1%), suggesting that their effects on sorption were somewhat diluted in the bulk soil. In other words, hexazinone and tebuthiuron will continue to pose groundwater contamination risks if biochars were applied at reasonable agricultural field rates, especially to sandy soils. Exceedingly high biochar application rates would be needed to effectively mitigate leaching of these highly mobile herbicides to groundwaters (Rittenhouse et al., 2014), or some alternate application strategy, such as either slight incorporation (at few centimeters) or horizontal band application beneath soil surface, working as a physical-chemical barrier preventing herbicides leaching (Jones et al., 2011). Amending high biochar rates ($\gg 10{,}000$ kg ha^{-1}) to soils seem not to be feasible for agronomical purposes, but it would still be a sustainable strategy to remediate priceless agricultural areas contaminated with highly mobile pesticides, especially those located in watershed recharge areas.

4.3. Sorption as affected by herbicide aging and biochar granulometry

Pesticide aging enhanced sorption in biochar amended soils, mainly for tebuthiuron, meaning that the ternary biochar-soil-pesticide associations enhance with time. The simultaneous "aging" of the biochar in amended soils may cause pore-clogging and biochar sealing by the soil particles, thus reducing its available SSA and its sorption potential (Khorram et al., 2017; Liu et al., 2018); but it was not the case. On the other hand, aging may have favored pesticide diffusion to less accessible sorption sites of the soils (Giori et al., 2014) and biochars (Kookana, 2010), thus increasing its sequestration. Ignoring aging for highly mobile herbicides may erroneously overestimate their leaching potentials.

Biochar granulometry did not consistently affect hexazinone and tebuthiuron retention, but finer particles (<0.15 mm) seemed to favor their sorption, mainly after aging. The literature showed similar results for less mobile molecules (Gao and Wu, 2013; Gelardi et al., 2019; Kang et al., 2018). For PM350, this trend was less evident due to the higher dissolution of its organic fraction. Although finely ground biochars usually present higher sorption (Kang et al., 2018); they are easily transported over long distances and can cause air pollution when pulverized to < 2.5 μm, thus harming human health (Gao and Wu, 2013; Gelardi et al., 2019).

5. Conclusions

The pore size distribution and SSA of biochars were successfully determined by a new low field NMR-DDIF method, in an unprecedented way in the literature for biochar, and it was pivotal to explain their potential to sorb highly mobile herbicides. The SSs, RHs, and PM650 were the most whereas SW and PM350 were the least effective sorbents to both hexazinone and tebuthiuron. Biochar macropores (diameter >5 μm) enhanced with pyrolysis temperatures and their SSAs seemed to modulate retention of these highly mobile herbicides. Biochar granulometry played a minor role, but pesticide aging increased retention and should be important to predict herbicide leaching in biochar amended soils. When synthesized at high pyrolysis temperatures, agroindustrial biochars can retain highly mobile herbicides. However, exceedingly high rates, or proper incorporation strategies, *i.e.*, light surface incorporation or subsurface horizontal band application, must be regarded to preclude these herbicides from leaching to groundwaters.

E-supplementary data of this work can be found in online version of the paper.

Declaration of competing interest

The authors declare that they have no known competing financial interests or personal relationships that could have appeared to influence the work reported in this paper.

Acknowledgments

Appendix A. Supplementary data

Supplementary data to this article can be found online at https://doi.org/10.1016/j.chemosphere.2021.132237.

Authors' contributions

LP contributed to data collection, analysis, and manuscript writing. EHN contributed to Nuclear Magnetic Resonance (NMR) spectroscopy data collection, analysis, and manuscript writing and review. CEPC contributed to Scanning Electron Microscopy (SEM) data collection, biochar manufacture, and manuscript review. AJS contributed to data analysis and manuscript review. BBM contributed to NMR data collection and analysis. VTL contributed to radiometric test assembles and data collection. JBR contributed to study design, funding acquisition, data analysis, manuscript writing, and overall project coordination.

Funding

References

Ahmad, M., Rajapaksha, A.U., Lim, J.E., Zhang, M., Bolan, N., Mohan, D., Vithanage, M., Lee, S.S., Ok, Y.S., 2014. Biochar as a sorbent for contaminant management in soil and water: a review. Chemosphere 99, 19–33. https://doi.org/10.1016/j.chemosphere.2013.10.071.

Albuquerque, A.F., Ribeiro, J.S., Kummrow, F., Nogueira, A.J.A., Montagner, C.C., Umbuzeiro, G.A., 2016. Pesticides in Brazilian freshwaters: a critical review. Environ. Sci. Process. Impacts. 18, 779–787. https://doi.org/10.1039/c6em00268d.

Benavides, F., Leiderman, R., Souza, A., Carneiro, G., Azeredo, R.B.V., 2020. Pore size distribution from NMR and image based methods: a comparative study. J. Petrol. Sci. Eng. 184, 106321. https://doi.org/10.1016/j.petrol.2019.106321.

Benavides, F., Leiderman, R., Souza, A., Carneiro, G., Bagueira, R., 2017. Estimating the surface relaxivity as a function of pore size from NMR T$_2$ distributions and microtomographic images. Comput. Geosci. 106, 200–208. https://doi.org/10.1016/j.cageo.2017.06.016.

Boesten, J.J.T.I., 2017. Effects of aged sorption on pesticide leaching to groundwater simulated with PEARL. Sci. Total Environ. 576, 498–507. https://doi.org/10.1016/j.scitotenv.2016.10.099.

Brewer, C.E., Chuang, V.J., Masiello, C.A., Gonnermann, H., Gao, X., Dugan, B., Driver, L.E., Panzacchi, P., Zygourakis, K., Davies, C.A., 2014. New Approaches to Measuring Biochar Density and Porosity. Biomass Bioenerg. https://doi.org/10.1016/j.biombioe.2014.03.059.

Cabrera, A., Cox, L., Spokas, K., Hermosín, M.C., Cornejo, J., Koskinen, W.C., 2014. Influence of biochar amendments on the sorption–desorption of aminocyclopyrachlor, bentazone and pyraclostrobin pesticides to an agricultural soil. Sci. Total Environ. 470, 438–443. https://doi.org/10.1016/j.scitotenv.2013.09.080, 471.

Cerdeira, A.L., Dos Santos, N.A.G., Pessoa, M.C.P.Y., Gomes, M.A.F., Lanchote, V.L., 2005. Herbicide leaching on a recharge area of the Guarany aquifer in Brazil. J. Environ. Sci. Heal. B. 159–165 https://doi.org/10.1081/PFC-200034294.

Chencarek, B., 2021. High-field Relaxation and Diffusion NMR Studies Applied to the Characterization of Confined Fluids. Thesis. Brazilian Center for Research in Physics, Rio de Janeiro.

Chencarek, B., Nascimento, M.S., Souza, A.M., Sarthour, R.S., Santos, B.C.C., Correia, M.D., Oliveira, I.S., 2019. Multi-exponential analysis of water NMR spin–spin relaxation in porosity/permeability-controlled sintered glass. Appl. Magn. Reson. 50, 211–225. https://doi.org/10.1007/s00723-018-1050-x.

Conte, P., Hanke, U.M., Marsala, V., Cimò, G., Alonzo, G., Glaser, B., 2014. Mechanisms of water interaction with pore systems of hydrochar and pyrochar from poplar forestry waste. J. Agric. Food Chem. 62, 4917–4923. https://doi.org/10.1021/jf5010034.

Conz, R.F., 2015. Caracterização de matérias-primas e biochars para aplicação na agricultura. Escola Superior de Agricultura Luiz de Queiroz/Universidade de São Paulo, Piracicaba. https://doi.org/10.11606/D.11.2015.tde-13052015-142608.

Conz, R.F., Abbruzzini, T.F., de Andrade, C.A., Milori, P., D M B, E.P., Cerri, C., 2017. Effect of pyrolysis temperature and feedstock type on agricultural properties and stability of biochars. Agric. Sci. 8, 914–933. https://doi.org/10.4236/as.2017.89067.

De Pasquale, C., Marsala, V., Berns, A.E., Valagussa, M., Pozzi, A., Alonzo, G., Conte, P., 2012. Fast field cycling NMR relaxometry characterization of biochars obtained from an industrial thermochemical process. J. Soils Sediments 12, 1211–1221. https://doi.org/10.1007/s11368-012-0489-x.

Dechene, A., Rosendahl, I., Laabs, V., Amelung, W., 2014. Sorption of polar herbicides and herbicide metabolites by biochar-amended soil. Chemosphere 109, 180–186. https://doi.org/10.1016/j.chemosphere.2014.02.010.

Delwiche, K.B., Lehmann, J., Walter, M.T., 2014. Atrazine leaching from biochar-amended soils. Chemosphere 95, 346–352. https://doi.org/10.1016/j.chemosphere.2013.09.043.

Deng, H., Feng, D., He, J., Li, F., Yu, H., Ge, C., 2017. Influence of biochar amendments to soil on the mobility of atrazine using sorption-desorption and soil thin-layer chromatography. Ecol. Eng. 99, 381–390. https://doi.org/10.1016/j.ecoleng.2016.11.021.

Egbosiuba, T.C., Abdulkareem, A.S., Kovo, A.S., Afolabi, E.A., Tijani, J.O., Auta, M., Roos, W.D., 2020. Ultrasonic enhanced adsorption of methylene blue onto the optimized surface area of activated carbon: adsorption isotherm, kinetics and thermodynamics. Chem. Eng. Res. Des. 153, 315–336. https://doi.org/10.1016/j.cherd.2019.10.016.

Gao, X., Wu, H., 2013. Aerodynamic properties of biochar particles: effect of grinding and implications. Environ. Sci. Technol. Lett. 1, 60–64. https://doi.org/10.1021/ez400165g.

Gelardi, D.L., Li, C., Parikh, S.J., 2019. An emerging environmental concern: biochar-induced dust emissions and their potentially toxic properties. Sci. Total Environ. https://doi.org/10.1016/j.scitotenv.2019.05.007.

Giori, F.G., Tornisielo, V.L., Pellegrino Cerri, C.E., Regitano, J.B., 2014. Sugarcane straw management and soil attributes on alachlor and diuron sorption in highly weathered tropical soils. J. Environ. Sci. Heal. B. 49, 352–360. https://doi.org/10.1080/03601234.2014.882172.

Gray, M., Johnson, M.G., Dragila, M.I., Kleber, M., 2014. Water uptake in biochars: the roles of porosity and hydrophobicity. Biomass Bioenergy 61, 196–205. https://doi.org/10.1016/j.biombioe.2013.12.010.

Haberhauer, G., Temmel, B., Gerzabek, M.H., 2002. Influence of dissolved humic substances on the leaching of MCPA in a soil column experiment. Chemosphere 46, 495–499. https://doi.org/10.1016/S0045-6535(01)00194-1.

Hassan, M., Liu, Y., Naidu, R., Parikh, S.J., Du, J., Qi, F., Willett, I.R., 2020. Influences of feedstock sources and pyrolysis temperature on the properties of biochar and functionality as adsorbents: a meta-analysis. Sci. Total Environ. https://doi.org/10.1016/j.scitotenv.2020.140714.

Herath, I., Kumarathilaka, P., Al-Wabel, M.I., Abduljabbar, A., Ahmad, M., Usman, A.R.A., Vithanage, M., 2016. Mechanistic modeling of glyphosate interaction with rice husk derived engineered biochar. Microporous Mesoporous Mater. 225, 280–288. https://doi.org/10.1016/j.micromeso.2016.01.017.

IBI, 2015. Standardized Product Definition and Product Testing Guidelines for Biochar that Is Used in Soil (Aka IBI Biochar Standards). International Biochar Initiative, Washington, D.C.

Inyang, M., Dickenson, E., 2015. The potential role of biochar in the removal of organic and microbial contaminants from potable and reuse water: a review. Chemosphere 134, 232–240. https://doi.org/10.1016/j.chemosphere.2015.03.072.

Jin, J., Kang, M., Sun, K., Pan, Z., Wu, F., Xing, B., 2016. Properties of biochar-amended soils and their sorption of imidacloprid, isoproturon, and atrazine. Sci. Total Environ. 550, 504–513. https://doi.org/10.1016/j.scitotenv.2016.01.117.

Jones, D.L., Edwards-Jones, G., Murphy, D.V., 2011. Biochar mediated alterations in herbicide breakdown and leaching in soil. Soil Biol. Biochem. 43, 804–813. https://doi.org/10.1016/j.soilbio.2010.12.015.

Kang, S., Jung, J., Choe, J.K., Ok, Y.S., Choi, Y., 2018. Effect of biochar particle size on hydrophobic organic compound sorption kinetics: applicability of using representative size. Sci. Total Environ. 619–620, 410–418. https://doi.org/10.1016/j.scitotenv.2017.11.129.

Khorram, M.S., Lin, D., Zhang, Q., Zheng, Y., Fang, H., Yu, Y., 2017. Effects of aging process on adsorption–desorption and bioavailability of fomesafen in an agricultural soil amended with rice hull biochar. J. Environ. Sci. 56, 180–191. https://doi.org/10.1016/j.jes.2016.09.012.

Kookana, R.S., 2010. The role of biochar in modifying the environmental fate, bioavailability, and efficacy of pesticides in soils: a review. Soil Res. 48, 627–637. https://doi.org/10.1071/SR10007.

Li, S., Lü, J., Zhang, T., Cao, Y., Li, J., 2017. Relationship between biochars' porosity and adsorption of three neutral herbicides from water. Water Sci. Technol. 75, 482–489. https://doi.org/10.2166/wst.2016.535.

Lisitza, N.V., Song, Y.-Q., 2001. The behavior of diffusion eigenmodes in the presence of internal magnetic field in porous media. J. Chem. Phys. 114, 9120–9124. https://doi.org/10.1063/1.1368659.

Liu, H., Nogueira D'Eurydice, M., Obruchkov, S., Galvosas, P., 2014. Determining pore length scales and pore surface relaxivity of rock cores by internal magnetic fields modulation at 2 MHz NMR. J. Magn. Reson. 246, 110–118. https://doi.org/10.1016/j.jmr.2014.07.005.

Liu, Y., Lonappan, L., Brar, S.K., Yang, S., 2018. Impact of biochar amendment in agricultural soils on the sorption, desorption, and degradation of pesticides: a review. Sci. Total Environ. 645, 60–70. https://doi.org/10.1016/j.scitotenv.2018.07.099.

Lowell, S., Shields, J.E., Thomas, M.A., Thommes, M., 2004. Characterization of Porous Solids and Powders: Surface Area, Pore Size and Density. https://doi.org/10.1007/978-1-4020-2303-3_1.

Mandal, A., Singh, N., Purakayastha, T.J., 2017a. Characterization of pesticide sorption behaviour of slow pyrolysis biochars as low-cost adsorbent for atrazine and imidacloprid removal. Sci. Total Environ. 577, 376–385. https://doi.org/10.1016/j.scitotenv.2016.10.204.

Mandal, S., Sarkar, B., Igalavithana, A.D., Ok, Y.S., Yang, X., Lombi, E., Bolan, N., 2017b. Mechanistic insights of 2,4-D sorption onto biochar: influence of feedstock materials and biochar properties. Bioresour. Technol. 246, 160–167. https://doi.org/10.1016/j.biortech.2017.07.073.

Mendes, K.F., Wei, M.C.F., Furtado, I.F., Takeshita, V., Pissolito, J.P., Molin, J.P., Tornisielo, V.L., 2021. Spatial distribution of sorption and desorption process of ^{14}C-radiolabelled hexazinone and tebuthiuron in tropical soil. Chemosphere 264–128494, 1–11. https://doi.org/10.1016/j.chemosphere.2020.128494.

Mukhtar, A., Mellon, N., Saqib, S., Lee, S.-P., Bustam, M.A., 2020. Extension of BET theory to CO2 adsorption isotherms for ultra-microporosity of covalent organic polymers. SN Appl. Sci. 2, 1232. https://doi.org/10.1007/s42452-020-2968-9.

Novotny, E.H., Maia, C.M.B., de, F., Carvalho, M.T., de, M., Madari, B.E., 2015. Biochar: carbono pirogênico para uso agrícola - Uma revisão crítica. Rev. Bras. Cienc. do Solo 39, 321–344. https://doi.org/10.1590/01000683rbcs20140818.

OECD, 2000. Test No. 106: adsorption-desorption using a batch equilibrium method. In: OECD Guidelines for the Testing of Chemicals, Section 1, OECD Guidelines for the Testing of Chemicals, Section 1. OECD, Paris. https://doi.org/10.1787/9789264069602-en.

Oliveira, F.R., Patel, A.K., Jaisi, D.P., Adhikari, S., Lu, H., Khanal, S.K., 2017. Environmental Application of Biochar: Current Status and Perspectives, vol. 246, pp. 110–122. https://doi.org/10.1016/j.biortech.2017.08.122. Bioresour. Technol.

Pereira-Junior, E.V., Giori, F.G., Nascimento, A.L., Tornisielo, V.L., Regitano, J.B., 2015. Effects of soil attributes and straw accumulation on the sorption of hexazinone and tebuthiuron in tropical soils cultivated with sugarcane. J. Environ. Sci. Heal. B. 50, 238–246. https://doi.org/10.1080/03601234.2015.999588.

Raij, B. van, Andrade, J.C. de, Cantarella, H., Quaggio, J.A., 2001. Análise química para avaliação da fertilidade de solos tropicais. Instituto Agronômico, Campinas.

Rémond, S., Gallias, J.L., Mizrahi, A., 2008. Characterization of voids in spherical particle systems by Delaunay empty spheres. Granul. Matter 10, 329–334. https://doi.org/10.1007/s10035-008-0092-4.

Rittenhouse, J.L., Rice, P.J., Spokas, K.A., Koskinen, W.C., 2014. Assessing biochar's ability to reduce bioavailability of aminocyclopyrachlor in soils. Environ. Pollut. 189, 92–97. https://doi.org/10.1016/j.envpol.2014.02.022.

Siedt, M., Schäffer, A., Smith, K.E.C., Nabel, M., Roß-Nickoll, M., van Dongen, J.T., 2021. Comparing straw, compost, and biochar regarding their suitability as agricultural soil amendments to affect soil structure, nutrient leaching, microbial communities, and the fate of pesticides. Sci. Total Environ. 751, 141607. https://doi.org/10.1016/j.scitotenv.2020.141607.

Song, Y.-Q., 2003. Using internal magnetic fields to obtain pore size distributions of porous media. Concepts Magn. Reson. 18A, 97–110. https://doi.org/10.1002/cmr.a.10072.

Song, Y.Q., Ryu, S., Sen, P.N., 2000. Determining multiple length scales in rocks. Nature 406, 178–181. https://doi.org/10.1038/35018057.

Sun, H., Hockaday, W.C., Masiello, C.A., Zygourakis, K., 2012. Multiple controls on the chemical and physical structure of biochars. Ind. Eng. Chem. Res. 51, 1587–1597. https://doi.org/10.1021/ie201309r.

Tan, X., Liu, Y., Zeng, G., Wang, X., Hu, X., Gu, Y., Yang, Z., 2015. Application of biochar for the removal of pollutants from aqueous solutions. Chemosphere 125, 70–85. https://doi.org/10.1016/j.chemosphere.2014.12.058.

Teixeira, P.C., Donagemma, G.K., Fontana, A., Teixeira, W.G., 2017. Manual de Métodos de Análise de Solo. EMBRAPA, Brasília.

Toniêto, T.A.P., de Pierri, L., Tornisielo, V.L., Regitano, J.B., 2016. Fate of tebuthiuron and hexazinone in green-cane harvesting system. J. Agric. Food Chem. 64, 3960–3966. https://doi.org/10.1021/acs.jafc.5b04665.

Tsai, W.T., Chen, H.R., 2013. Adsorption kinetics of herbicide paraquat in aqueous solution onto a low-cost adsorbent, swine-manure-derived biochar. Int. J. Environ. Sci. Technol. 10, 1349–1356. https://doi.org/10.1007/s13762-012-0174-z.

Wang, J., Shi, L., Zhai, L., Zhang, H., Wang, S., Zou, J., Shen, Z., Lian, C., Chen, Y., 2021. Analysis of the long-term effectiveness of biochar immobilization remediation on heavy metal contaminated soil and the potential environmental factors weakening the remediation effect: a review. Ecotoxicol. Environ. Saf. 207, 111261. https://doi.org/10.1016/j.ecoenv.2020.111261.

Wang, Z., Han, L., Sun, K., Jin, J., Ro, K.S., Libra, J.A., Liu, X., Xing, B., 2016. Sorption of four hydrophobic organic contaminants by biochars derived from maize straw, wood dust and swine manure at different pyrolytic temperatures. Chemosphere 144, 285–291. https://doi.org/10.1016/j.chemosphere.2015.08.042.

Wong, J.W.C., Webber, J.B.W., Ogbonnaya, U.O., 2019. Characteristics of biochar porosity by NMR and study of ammonium ion adsorption. J. Anal. Appl. Pyrolysis 143, 104687. https://doi.org/10.1016/j.jaap.2019.104687.

Xiao, F., Pignatello, J.J., 2015. Interactions of triazine herbicides with biochar: steric and electronic effects. Water Res. 80, 179–188. https://doi.org/10.1016/j.watres.2015.04.040.

Yavari, S., Malakahmad, A., Sapari, N.B., Yavari, S., 2016. Sorption-desorption mechanisms of imazapic and imazapyr herbicides on biochars produced from agricultural wastes. J. Environ. Chem. Eng. 4, 3981–3989. https://doi.org/10.1016/j.jece.2016.09.003.